ACS OMEGA

Open Access

This article is licensed under CC-BY-NC-ND 4.0

http://pubs.acs.org/journal/acsodf

Article

# Co-Pyrolysis of Date Palm Waste and *Salicornia Bigelovii*: Insights for Bioenergy Development in Arid and Semi-Arid Regions

Waqas Ahmad, Yassir Makkawi,* and Fatin Samara*

Cite This: *ACS Omega* 2024, 9, 24082−24094

Read Online

ACCESS | Metrics & More | Article Recommendations | Supporting Information

**ABSTRACT:** Bioenergy is predicted to significantly contribute to the global energy needs of both developed and developing economies. Co-pyrolysis of halophytes offers a solution for a sustainable supply of feedstock in coastal and water-scarce regions. This novel research introduces an experimental investigation of co-pyrolysis of saline-tolerant flora (date palm waste and *Salicornia bigelovii*) to address sustainable waste management, bioenergy production, and efficient resource utilization in xeric regions. To examine the impact of the thermic condition on the pyrolysis products (bio-oil, biochar, and gas), the experiments have been conducted at three different temperatures (400, 500, and 600 °C). This pioneering study revealed that the co-feed bio-oil is acidic (pH 3.76−4.39) and has a high energy content (HHV 32.29−36.29 MJ/kg) that surpasses most woody biomass. The produced biochar was chemically stable, high in ash (40.09−47.62 wt %), high in fixed carbon (30.12−38.12 wt %), highly alkaline (pH 9.37−10.69), and low in HHV (16.30−17.2 MJ/kg). Increased pyrolysis temperature enhances biochar stability and fixed carbon, thus benefiting long-term carbon sequestration if applied in the soil. However, due to its high alkalinity, the application of this biochar in naturally alkaline sandy soils, such as in coastal deserts, requires careful monitoring. The hydrogen content in the gaseous phase significantly improves with rising temperature, reaching HHV = 24.12 MJ/kg at 600 °C, due to the enhanced ash catalytic effect. Overall, this study constitutes an important contribution to advancing bioenergy, sustainable feedstock, carbon capture, and waste management strategies in drought-prone areas.

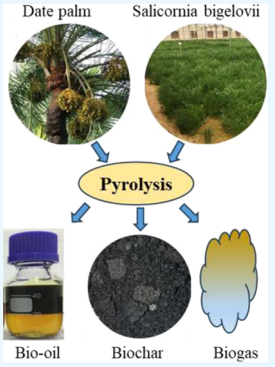


## 1. INTRODUCTION

Environmental obstacles linked with the utilization of conventional fuels[1] have led to an increase in demand for more efficient renewable and green energy sources. Among the currently available renewable energy sources, biomass presents a high potential to meet the energy demands of modern societies in developed and developing economies.[2] It is projected that by the year 2050, biomass will have the capability to generate 3000 terawatt-hours (TWh) of electricity, leading to an annual reduction of 1.3 billion metric tons of $CO_2$ equivalent emissions.[2,3]

As part of sustainable power solutions, biomass can be converted to energy via thermal, biological, and physical methods. Thermal conversion through pyrolysis has attracted considerable interest owing to the broad range of potential applications for its resulting products, including bio-oil, gas, and biochar.[4−7] The thermal conversion process involves the decomposition of biomass or general organic matter in a controlled inert environment, breaking the material into a pyrolysis effluent: vapor and biochar. After condensation, the pyrolysis vapor reduces to an organic liquid and an uncondensed gas (NCG). The quality of the resulting products during the thermal degradation is primarily controlled by two main factors: the temperature at which pyrolysis occurs and the type of feedstock used.[8] For this reason, optimizing the temperature and feedstock composition is essential to attain the intended quality of products. For instance, a balance must be struck between maximizing carbon content and ensuring biochar's suitability for its intended use, which includes but is not limited to carbon sequestration, soil modification, and energy.[9] The bio-oil or liquid produced through this process is characterized by its rich content of organic chemical compounds. Depending on the feedstock composition and pyrolysis temperature, the yielded bio-oil can undergo additional refinement processes to achieve a higher fuel quality and use as raw material for chemical production.[10−12] Similarly, the pyrolysis gas includes a wide range of gases, including hydrogen and carbon monoxide, and its heating value can vary significantly with the feedstock composition and pyrolysis temperature.

The importance of the feedstock or biomass material used for the pyrolysis process is of main interest, as previously mentioned. The United Arab Emirates (UAE) has a hyper-arid climate; hence, halophytes such as *Salicornia bigelovii* grown in arid lands using saltwater are a good choice for biomass material. Moreover, the UAE and the whole MENA[13] have an

Received: March 28, 2024
Revised: May 7, 2024
Accepted: May 15, 2024
Published: May 22, 2024

© 2024 The Authors. Published by American Chemical Society

**Table 1. Literature on Pure Date Palm and *S. bigelovii* Pyrolysis**

| materials study | sample location/type | approach/reactor used | main findings | refs |
|---|---|---|---|---|
| date palm waste mixture | Sharjah, UAE | fluidized bed reactor<br>temperature: 525 °C | yield (38.8% heavy phase, 37.2% biochar, 24 NCG%).<br>date palm mixture shows significant ash, elevated oxygen, low volatile, and average HHV. | 22 |
| date palm seeds | Rabigh, Saudi Arabia | fixed bed reactor<br>temperature: 400, 600, 800, 1000 °C | focused on biochar and syngas.<br>get 97.99% of total carbon content at 800 °C.<br>highest syngas at 1000 °C i.e., 40 mol % H2 and 32 mol % CO.<br>kinetic analysis indicated activation energy of 30−40 kJ/mol. | 32 |
| *S. bigelovii* and Date palm | Salicornia full plant and date palm leaves from Abu Dhabi UAE. | thermogravimetric analysis 1:1 mixed. | performed kinetic analysis.<br>the activation energy for *S.bigelovii* and date palm is 147.6 and 164.7 kJ/mol. | 31 |
| date palm and Pistachio | date palm leaves and branches from Jiroft, Iran. Pistachio upper stem from Neyriz, Iran. | fixed stainless steel tube furnace. temperature: 500 °C, at argon atmosphere. 60:40 mixed | Co-pyrolysis improves properties like reduced ash content HBC 18.68% compared to 28.11% DBC, and increased carbon content 66.1% as compared to 49.33% DBC. | 33 |
| date palm leaves | Abu Dhabi,UAE | furnace, temperature: 300, 400, 500, and 600 °C<br>for $CO_2$ sequestration fluidized bed reactor is used. | the $CO_2$ captured at 300, 400, 500, and 600 °C is 7, 9, 15, 20, and 25%. | 20 |
| date palm waste | fronds, and leaves | electric muffle furnace, temperature: 400, 500, and 600 °C | biochar lost functional groups with temperature rise.<br>surface area increased which leads to higher removal efficiencies (98−100%) of Ni, Fe, Zn, and Cu at pH > 6. | 34 |
| Vegetation *S. bigelovii* (water wash pretreatment sample, and untreated) | Greenhouse, KAUST, Saudi Arabia | quartz tube reactor. temperature: 600, 700, and 800 °C | yield bio-oil produced at 700 °C for pretreated Salicornia is 25% higher than the untreated sample.<br>highest biochar yield at 600 °C for untreated, 45.7% compared to 36.7% for treated. | 35 |
| Co-pyrolysis *S. bigelovii* and Heavy fuel oil (HFO) | Salicornia from KAUST, Saudi Arabia, and HFO from a station with 31 wt % diesel and 69 wt % vacuum residual oil | quartz tube reactor, $N_2$ environment. temperature: 550 °C | 75% HFO Co-pyrolysis promotes cracking and volatilization leading to high gas yield and reduced biochar.<br>bio-oil GCMS data shows an improvement in aliphatic and aromatic hydrocarbons and reduced carboxylic acids by 34%. | 36 |
| *S. bigelovii* | SBRC, Abu Dhabi, UAE | muffle furnace. temperature: 350 °C | biocahr pH = 8.6 and BET 1.72 $m^2/g$ used for sandy soil amendment. | 37 |



https://doi.org/10.1021/acsomega.4c02972
ACS Omega 2024, 9, 24082−24094

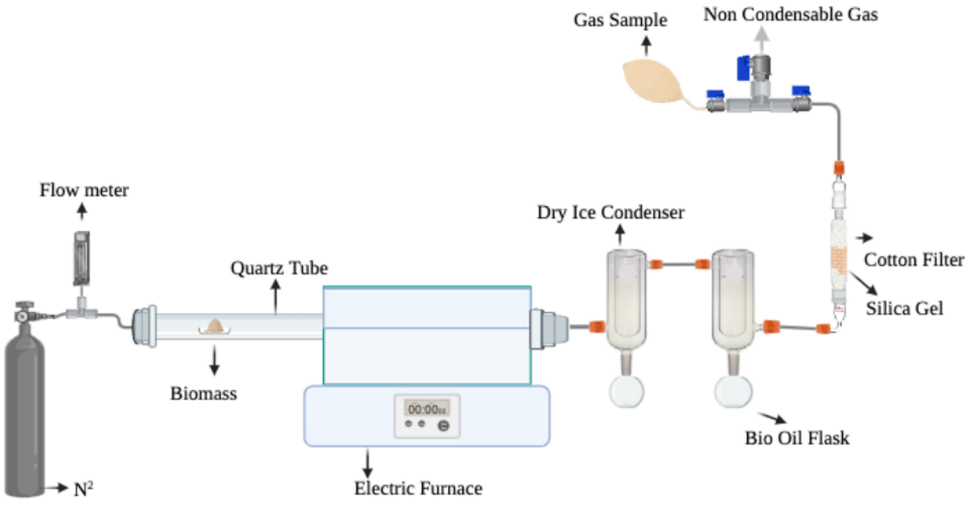


**Figure 1.** Schematic illustration of the batch tubular reactor and the pyrolysis vapor condensation setup.

abundance of agricultural residues of date palms,[14] which is indigenous dry terrain halophyte. *S. bigelovii*, which shall be referred to as *Salicornia* for simplicity, is reported to have originated in the Mediterranean Basin and is considered to enhance sustainable agriculture due to its salt-tolerance characteristic, which alleviates the strain on freshwater resources.[15] Date palm tree[16] is an alternative classification of halophilic flora that thrives in challenging habitats[17] (saline water and hot temperatures) and is cultivated for its edible fruit naturalized in tropical and subtropical regions worldwide.[18] In the MENA realm,[19] the date palm tree is the most prevalent agricultural crop, contributing approximately 2.8 million tons of waste annually.[13] The UAE annual production of date palm waste exceeds 0.5 million tons,[20] making the thermal decomposition of this biomass a promising venue to switch these remains instead of being discarded in landfills.[21] Both types of plants, date palm and Salicornia, have garnered attention as mono feedstocks for multiple applications, though in limited numbers compared to other types of woody biomass. The summary of the latest studies[22] on date palm waste and *Salicornia* pyrolysis during the past 6 years is shown in Table 1. The literature indicated the promising utilization[23] of the pyrolysis yields in bioenergy production,[14,23−26] carbon sequestration,[25,27,28] and soil enhancement.[28,29]

Despite their potential for bioenergy applications, there is limited literature on the transformation of date palm waste through pyrolysis[30] and *Salicornia* as co-feed. One study reported results on co-feeding date palm waste and Salicornia but this was only focused on deriving the pyrolysis kinetics through the thermogravimetric analysis (TGA) analysis.[31] Therefore, this study marks a pioneering effort in exploring the co-pyrolysis process involving date palm waste and Salicornia, contributing significantly to advancing sustainable waste management and resource utilization strategies in xeric regions. A key focus of this research lies in conducting a comprehensive examination of how varying pyrolysis temperatures impact the properties and chemical composition of the resulting products, with particular emphasis on their potential applications in energy generation, carbon sequestration, and soil improvement. The decision to employ a 1:1 mixing ratio serves as a strategic starting point to maximize output and effectively address the challenge of high waste generation. While not conclusively established as the optimum co-feeding ratio, this balanced ratio allows for an equal representation of both date palm waste and Salicornia in the co-feed mixture, facilitating a thorough assessment of their combined pyrolysis behavior. Moreover, the deliberate choice to investigate temperatures of 400, 500, and 600 °C enables insight into the optimal conditions for enhancing output and product quality. These selected temperatures were strategically chosen to cover a broad spectrum of pyrolysis conditions, aiming to capture potential changes in product composition and quality across different temperature regimes. Furthermore, this research extends beyond conventional bio-oil applications, exploring the broader benefits of co-pyrolysis and addressing a significant gap in the literature regarding the transformation of date palm waste and Salicornia through co-pyrolysis. The novelty of this research lies in its systematic investigation of the effects of pyrolysis temperature on the product characteristics from a new type of biomass mixture that has never been investigated in the past, thus offering promising avenues for more efficient biomass resource utilization, especially in arid regions.

## 2. EXPERIMENTAL PROCEDURES

**2.1. Feedstock and Pretreatment.** The Salicornia plant was obtained from experimental farms at the International Center for Biosaline Agriculture (ICBA)[38] in Dubai, UAE, and was watered using high-salinity water. The Phoenix dactylifera waste including plant leaves, leaf stems, and empty fruit bunches[39] was gathered from date palm trees cultivated in the American University of Sharjah (AUS) premises and was irrigated using municipality-treated wastewater. The date palm waste and Salicornia were air-dried for a few days with direct sunlight exposure at outdoor temperatures of approximately 40 °C. The dehydrated biomass was diced into small bits and processed into fragments using a cutting mill (Retsch - SM 200 model).[22] Using a vibrating shaker, these particles were then sieved to achieve a size range[40] of 0.5−1.0 mm (sieve opening). The co-feed was then prepared by mixing equal proportions to create a single feedstock.

**2.2. Experiment Setup and Procedure.** A diagram representation of the pyrolysis setup used in this study is shown in Figure 1, and the operating conditions are shown in Table 2. Briefly, the setup is divided into the batch tube reactor, the gas condensation, and the liquid (bio-oil and aqueous phases) collection. The initial segment of the system


https://doi.org/10.1021/acsomega.4c02972
ACS Omega 2024, 9, 24082−24094

Table 2. Summary of the Operating Conditions of the Batch Tubular Reactor

| parameter | experiment condition |
|---|---|
| sweeping gas (nitrogen) | |
| inlet temperature (°C) | 25 |
| flow rate (ml $min^{-1}$) | 400−700 |
| biomass | |
| Co-feed mixing ratio | 1:1 |
| average particle size (mm) | 0.294 |
| fixed bed sample weight (g) | 65 |
| reactor | |
| sample holder dimensions (cm) | 10.0 length, 4.2 diameter |
| operation mode | fixed bed |
| temperature (°C) | 400−600 |
| heating power (W) | 1200 |

represents the pyrolysis reactor where biomass is introduced through a stainless-steel boat, which serves as a carrier for the biomass during the reaction, and a container for the resulting biochar postpyrolysis. The boat is positioned inside a quartz tube with high resistance to temperatures up to 1100 °C. An electric furnace (Type: CHY-T1200) is used to heat the quartz tube. A thermocouple is placed inside the furnace near the quartz tube, ensuring continuous monitoring and control of the pyrolysis temperature. The gas condensation section is connected to the end of the quartz tube consisting of dry ice condensers and round bottle flasks designed to collect bio-oil. The condenser's gas outlet is connected to a cotton filter and silica gel to clean the gas before it is discharged into a gas bag, collected for gas chromatography (GC) sampling, or released through a vent. Before the experiment is begun, nitrogen gas is introduced into the system as a sweeping gas to create and maintain the inert environment within the pyrolysis reaction zone.

At the start of the experiment, the biomass boat is loaded with around 65 g of biomass and positioned on the left cold side of the quartz tube, away from the heating zone of the furnace. A wire is connected to the end of the reactor and utilized to pull the biomass boat toward the middle of the furnace once the desired temperature is reached. The pyrolysis vapor passes through the dry ice condenser to produce the liquid in a collection flask and a noncondensable gas. At the end, the furnace tube is cooled to ambient temperature to collect the biochar from the boat.

The liquid product comprises two distinct phases: aqueous and heavy. The aqueous phase, characterized by its low viscosity and light color, stands in contrast to the heavy phase, known as bio-oil, which exhibits higher viscosity and a darker color. These two phases separate easily by gravity when placed in a separation funnel. To ensure precision in mass balance, glassware is weighed both before and after experimentation.

**2.3. Characterization Methods.** *2.3.1. Product Yield.* The pyrolysis product yield was assessed by collecting and determining the quantity of the products. To ensure accurate measurement of the pyrolysis products, the reactor tube, dry ice condenser, cotton filter, and liquid collection flasks were thoroughly inspected and weighed before and after the process. The amount of noncondensable gas (NCG) was estimated by the difference (NCG = Biomass-liquid-biochar). Each test was conducted 3 times to confirm the reproducibility. The yield proportion of the pyrolysis liquid, including bio-oil and aqueous components, and the biochar were calculated utilizing the subsequent equation

$$\text{yield } \% = \frac{\text{mass of product (biochar, bio-oil, NCG)}}{\text{mass of feed biomass}} \times 100 \quad (1)$$

*2.3.2. Proximate and Elemental Analysis.* Proximate analysis was performed to ascertain the water content, ash, and volatiles in both the feedstock and the biochar. The fixed carbon content (FCC) was determined by deducting the total water content, ash, and volatiles from 100%. The moisture content was determined according to standard protocol CEN/TS 14774−1:2004. The ash content was determined using the procedure outlined in CEN/TS 14775:2004 and the subsequent equation

$$\text{AC } \% = \left[\frac{m_1}{m_0} \times 100\right] \times \frac{100}{(100 - \text{MC}\%)} \quad (2)$$

In which $m_1$ denotes the mass of the sample post-treatment, $m_0$ is the mass of sample pretreatment, and MC% represents the water content percent. The volatiles are calculated using the standard procedure outlined in CEN/TS 15148:2005 and the following equation

$$\text{VC } \% = \left[\frac{100\,(m_0 - m_1)}{m_0} - \text{MC}\%\right] \times \left[\frac{100}{100 - \text{MC}\%}\right] \quad (3)$$

The ultimate analysis to assess the concentration of _C, _H, _N, and _S was carried out by employing an elemental analyzer. The oxygen matter was determined by a difference from 100%. The thermogravimetric analysis (TGA) was performed, applying a consistent ramp rate of 10 °C/min across the spectrum of 25−900 °C, with nitrogen gas employed as the carrier medium throughout the experimental procedure.

*2.3.3. Heating Value (HHV).* The HHV[22] of the feedstock and the products of pyrolysis were determined by an oxygen bomb calorimeter[41] (model: IKA C5003). The HHV of the noncondensable gas was determined based on the molar concentration of its flammable components as follows:[41]

$$\text{HHV}\left(\frac{\text{MJ}}{\text{Kg}}\right) = \sum_{i=1}^{n} (x_i \times \text{CV}) \quad (4)$$

where $i.\cdots n$ refer to each NCG component, $x_i$ is the mass fraction in the gas product, and CV is the calorific value of component gas in MJ/kg.

*2.3.4. Chemical Characterization of the Heavyweight Bio-Oil and NCG.* The constituents of the heavyweight bio-oil were analyzed using gas chromatography/mass spectrometry (GC/MS) (model: QP2010 Ultra Thermal Desorption, Shimadzu). For quantitative results, standard solutions n-tridecane and diglycerate were mixed with ethanol and the heavyweight bio-oil, before injection. The GC oven temperature program was initially set at 60 °C for 2.0 min hold time and at 5 °C/min to 300 °C held for 10 min. MSD source temperature was 230 °C and the GC column temperature was 280 °C. The naming of the chemical compounds was executed using NIST 2017 libraries, and the precision of each compound peak was validated manually. The noncondensable gas composition was analyzed using GC (Agilent 490 Micro GC system model)[40]


https://doi.org/10.1021/acsomega.4c02972
ACS Omega 2024, 9, 24082−24094

equipped with a gas dryer and two columns to detect lightweight gases, $CO_2$, $H_2$, CO, and $CH_4$, and heavyweight gases $C_2H_4$, $C_2H_6$, $C_3H_6$, $C_3H_8$, and $n$-$C_4H_{10}$.

*2.3.5. Acidity, Conductivity, and Salinity Analysis.* The pH and electrical conductivity (EC) of both the feedstock and biochar were determined by utilizing a digital meter (HI-5521−02 model). A 5.0 g amount of finely powdered feedstock and biochar was mixed in 50 mL of DI-water at 1:5, agitated via a magnetic stirrer for 1 h, and soaked for 30 min. The solid matter was isolated from the liquid employing vacuum filtration, and the pH, salinity, and EC were measured in the filtrate using pH probe (HI 1043B) and salinity and EC probe (model: HI 76312). The acidity level of the pyrolysis liquid, encompassing both organic and aqueous phases, was assessed by using a dedicated probe (HI 1043 model) for pH measurement.

*2.3.6. Surface Area and Morphology.* Scanning electron microscopy model (SEM, Tescan VEGA3 SEM, Czech Republic) combined with energy-dispersive X-ray spectroscopy (model: energy-dispersive system (EDS), Oxford Instruments INCA X-Act, United Kingdom)[41] was used to examine the top structure and elemental composition of the feedstock and biochar specimens. In preparation for the analysis, approximately 1 mg of the samples was positioned on carbon films attached to a metal stud, which was subsequently introduced into a vacuum environment. Prior to analysis, the specimens were coated with gold or platinum within a sputter chamber to ensure conductivity. SEM imaging and qualitative analysis of elemental composition using EDS was recorded. The samples' surface area was evaluated utilizing Brunauer−Emmett−Teller (BET) technique with the aid of a gas sorption analyzer (model: Autosorb-iQ32 Quantachrome) using liquid nitrogen ($N_2$) at −196.15 °C. Before analysis, the samples underwent preparation involving heating at 100 °C and degassing for approximately 4 h.

## 3. RESULTS AND DISCUSSION

**3.1. Feedstock Characteristics.** The results of the co-feed analysis are shown in Table 3. The proximate analysis showed a moisture content of 7.18%, a volatile matter content of 60.65%, an ash content of 20.3%, and a fixed carbon content of 11.9%. The elevated ash percentage in the mixture is primarily attributed to the existence of high ash in the individual feedstock, as reported by Makkawi et al. The arid climate of the UAE, which is limited in rainfall and has a high evaporation rate, contributes to increasing the inorganic elements in the soil, which subsequently accumulate in the plant leaves and stems as ash. Compared to the reported literature on the proximate analysis of Salicornia seed and seedless plant,[41] and that of date palm,[26] it is observed that the co-feed has lower volatiles but higher ash and fixed carbon content. High ash in the feedstock reduces its heating value, therefore, limiting its potential use as a solid fuel. The ultimate analysis results show that the co-feed has a similar composition in terms of C, H, S, N, and O content close to that is reported for the individual date palm and Salicornia plant feedstocks.[22,26,41] The co-feed mixture has a HHV of 14.93 MJ/kg, compared to 17.52 MJ/kg for the date palm waste and 13.27 MJ/kg for the Salicornia seedless plant. The estimated lignocellulosic composition of the co-feed reveals hemicellulose, cellulose, and lignin contents of 17.6, 32.2, and 24.9%, respectively, which is close to the reported data for date palm waste.[42]

**Table 3. Characteristics of the Co-Feed Biomass**

| | |
|---|---|
| proximate analysis (wt %) | |
| moisture | 7.18 ± 0.65 |
| volatiles | 60.65 ± 0.60 |
| fixed Carbon[a] | 11.88 |
| ash | 20.29 ± 0.25 |
| ultimate analysis (wt %) | |
| C | 33.67 |
| H | 3.65 |
| N | 0.88 |
| S | 0.24 |
| O[b] | 41.28 |
| hemicellulose (wt %) | 17.57 |
| cellulose (wt %) | 32.16 |
| lignin (wt %) | 24.87 |
| HHV (MJ/kg) | 14.93 |

[a]Fixed carbon = 100 − (Moisture + Ash + Volatile). [b]O% = 100% − (C% + H% + N% + S% + Ash%).

The TGA profiles presented in Figure 2 show the thermal decomposition behaviors of the date palm waste, Salicornia, and their co-feed sample. In general, the three profiles show similar trends. The onset of major mass loss is observed at around ∼190 °C and extends up to ∼550 °C. This is the range of temperature where major degradation of hemicellulose and cellulose decomposition takes place and is commonly referred to as the active pyrolysis stage.[43] The lignin predominantly decomposes at a higher temperature (>500 °C.), which is commonly referred to as passive pyrolysis stage; however, some of the lignin may also decomposes within the active pyrolysis stage. The proximate analysis presented in Table 3 aligns well with the observed TGA profiles. Initially, moisture is released up to around 25 to 110 °C; subsequently, a relatively thermally stable phase with minimal mass loss persists up to approximately 200 °C. Hemicellulose decomposition occurs within the range of 200 to 280 °C, followed by cellulose devolatilization and decomposition spanning 280 to 390 °C for date palm, whereas for salicornia and co-feed, devolatilization occurs up to 410 °C. Similar temperature ranges for significant devolatilization have been reported in the literature for plant-based biomass.[17,22,43−45]

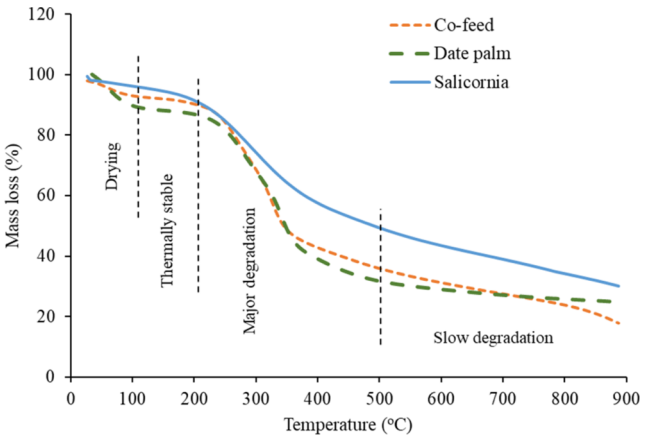


**Figure 2.** Thermogravimetric analysis (TGA) curves of date palm waste,[22] salicornia, and co-feed.


https://doi.org/10.1021/acsomega.4c02972
ACS Omega 2024, 9, 24082−24094

**3.2. Measurement of Pyrolysis Products.** The output yield obtained from pyrolyzing the co-feed mixture of Salicornia and date palm at 400, 500, and 600 °C is presented in Figure 3. This is presented in comparison to the distribution

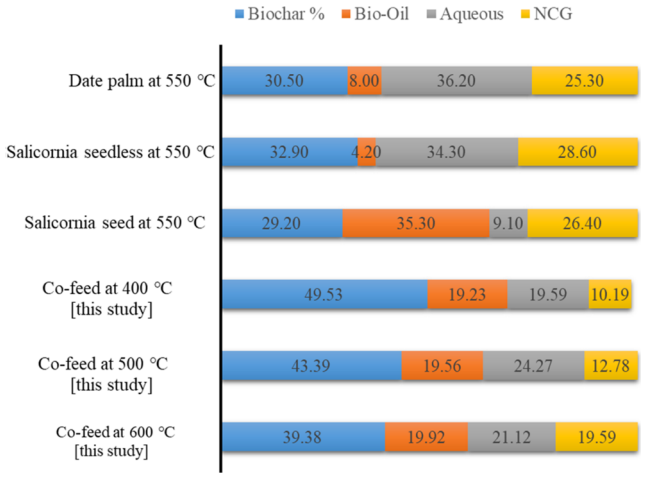


**Figure 3.** Distribution of the pyrolysis products from co-feed at different temperatures in comparison to pure feeding cases (date palm, Salicornia seed, and seedless plant) reported in the literature.[17,22,41]

of the pyrolysis product from the pure feedstocks. In the case of co-feeding, the results show that at a lower pyrolysis temperature of 400 °C, a higher biochar yield of 49.53% was produced, accompanied by a lower NCG yield of 10.19%. The substantial biochar yield at this temperature suggests a limited devolatilization. With the escalation of pyrolysis temperature from 400 to 600 °C, there is a progressive decline in biochar yield. This decline is likely due to the increased escape of volatile substances at elevated pyrolysis temperatures. These volatile components are converted into bio-oil through condensation, while noncondensable gases are collected in the gas bag. Simultaneously, the biochar decrease promotes the generation of heavyweight bio-oil and NCG. The generation of heavyweight bio-oil remains relatively unchanged, i.e., independent of temperature. However, NCG production exhibits an upward trend with increasing temperature, measuring 10.19, 12.78, and 19.59% at 400, 500, and 600 °C, correspondingly.

The results of pure feed pyrolysis as reported by Makkawi et al. revealed that the bio-oil yields from these feedstocks vary. When pyrolyzed at 550 °C, the bio-oil yields for Salicornia seed, Salicornia seedless plant, and date palm are found to be approximately 35.3, 7, and 8%, respectively. Among the biomass sources, Salicornia seed exhibited the highest bio-oil yield at 35.3%, while both date palm and Salicornia seedless plants exhibited bio-oil yields of less than 10% at 550 °C. Comparative results between pure biomasses and the co-feed mixture revealed significant differences. This result suggests that in the case of co-feeding, the pyrolysis is significantly affected by the presence of ash, coming from the salicornia plant and date palm waste, thus leading to a considerable decrease in heavyweight bio-oil yield. Additionally, the high ash content promotes gas dryness and the decomposition of cellulose fiber in biomass, resulting in the formation of water-soluble compounds that are redirected to the aqueous phase instead of being present in the bio-oil.

**3.3. Noncondensable Gas (NCG).** The components of the NCG and its HHV are shown in Figure 4. The figures illustrate the mass proportion of 4 primary lightweight gases, including _$H_2$, _CO, _$CO_2$, and_$CH_4$, in addition to 4 heavyweight gases within the $C_2$−$C_4$ range. The gases with the highest concentrations among all samples were CO and $CO_2$. Carbon dioxide was the predominant gas, and the findings unveiled that escalating the temperature led to a decrease in the gas with percentages of 69.34, 65.08, and 45.11% at temperatures of 400, 500, and 600 °C, correspondingly. The significant portion of $CO_2$ within the gas can mainly be linked to the increased oxygen content in the feedstock and potentially to the breakdown of organic matter facilitated by the ash. The $CO_2$ and CO are within the range reported for various types of feedstocks.[17] The levels of $H_2$ and $CH_4$ increase with increasing temperature, and this contributes to improving the gas HHV, especially at the pyrolysis temperature of 600 °C. Tar cracking may also contribute additional CO and $H_2$ to the gas. It is also plausible that the presence of a substantial amount of ash metal in the biochar enhances (catalyzes) the formation of $H_2$, $CH_4$, and CO. Another noteworthy observation is that the heavy gas mixtures ($C_2$−

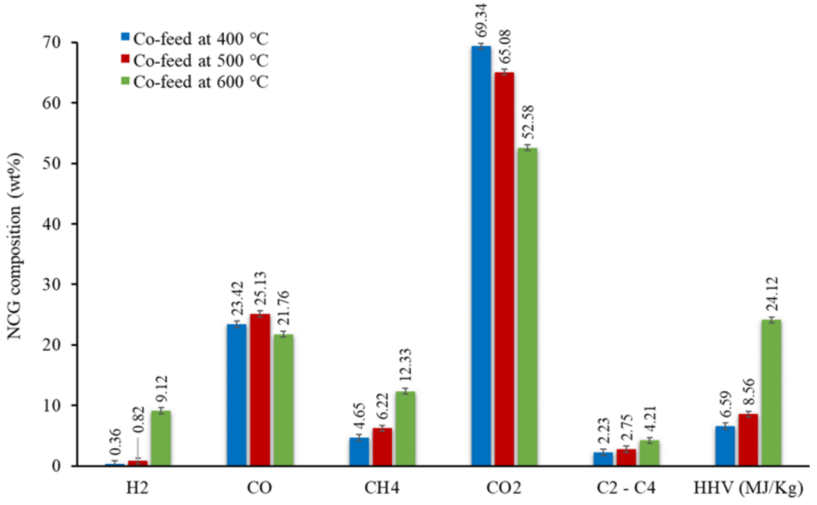


**Figure 4.** Chemical composition and HHV of NCG of the co-feed pyrolysis.


https://doi.org/10.1021/acsomega.4c02972
ACS Omega 2024, 9, 24082−24094

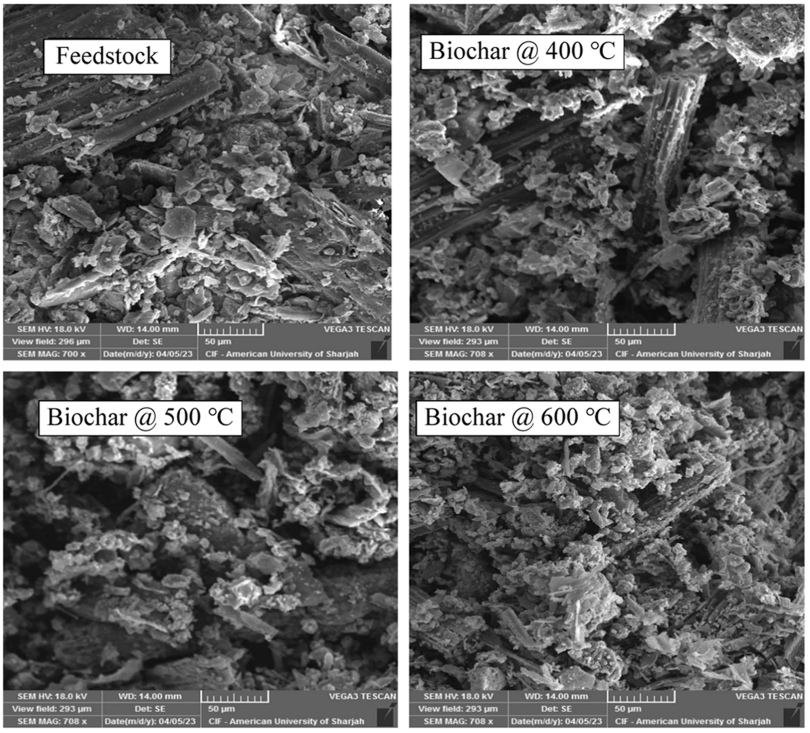


**Figure 5.** SEM images of the co-feed biomass and char at 400, 500, and 600 °C.

$C_4$) are mostly present in minimal concentrations (<5%). The existence of $C_2$−$C_4$ gases minimally affects the HHV of the NCG due to their comparatively minimal concentrations. The HHV values obtained in the co-feeding were 6.59, 8.56, and 24.12 MJ/kg at 400, 500, and 600 °C, correspondingly. Lower temperatures lead to a higher production of $CO_2$. As a result, the energy content of the co-feed at lower temperatures, 400 and 500 °C, is relatively low compared to fossil fuels. However, it is potentially adequate to supply the necessary heat to maintain the pyrolysis procedure. At the higher temperature of 600 °C, the co-feed exhibits a significantly higher energy content, approaching the energy content of fossil fuels, which is around 50 MJ/kg.[46] This increase in energy content is credited to the increased generation of $H_2$, CO, and $CH_4$ at the higher temperature of 600 °C.

**3.4. Characteristics of Biochar.** *3.4.1. Physical and Chemical Characteristics.* Scanning electron microscope (SEM) images, captured at identical levels of magnification, resolution, and power, depicted by the biochar samples are presented in Figure 5. Through visual examination of the images, there are no notable distinctions in the structure. However, the BET surface area, discussed in the next section, depicts a different picture.

The elemental composition of the char at the different pyrolysis temperatures was compared with that of the feedstock biomass, as shown in Figure 6. Notably, in all biochar samples, nitrogen content was significantly higher compared to other elements. Nitrogen values ranged from 30 to 59%. It is important to note that carbon, which serves as an adhesive material, and gold, utilized as a coating material, are intentionally excluded from the EDS analysis, to confirm the accurateness of the results. The second major element detected in all samples was chlorine (Cl), followed by the presence of several minor elements, for instance, Mg, Na, _Si, _Ca, _K, _and O. The presence of salts, potentially including sodium

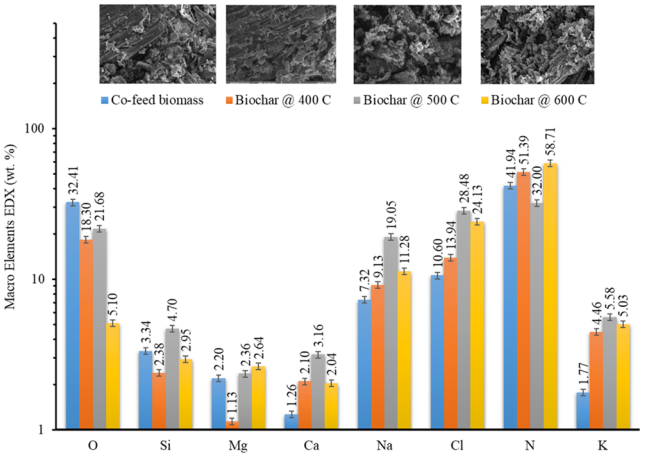


**Figure 6.** EDX elemental composition (normalized mass %) analysis of co-feed biomass and biochar produced at 400, 500, and 600 °C.

chloride (NaCl), magnesium chloride (MgCl), and calcium chloride ($CaCl_2$), is expected to be introduced by the saline irrigation water.

Proximate and elemental analyses were performed on the biochar samples and compared to the feedstock and reported literature as shown in Table 4. As expected, the findings indicate that as the temperature of pyrolysis increases, the moisture and volatile content drops. This decrease can be recognized to the discharge of moisture and volatiles, resulting in an increased concentration of ash and carbon through carbonization. The ashes and its features show a crucial part in determining the potential uses of biochar, such as its use as a solid fuel, soil remediation agent, water treatment medium, or catalyst. All feedstocks demonstrated a linear rise in the ash content as the temperature increased. The elemental analysis of _C, _H, _N, _S, and _O contents, along with FC and the


https://doi.org/10.1021/acsomega.4c02972
ACS Omega 2024, 9, 24082−24094

**Table 4. Proximate and Elemental Analysis of the PCM Produced by Co-Feeding at 400, 500, and 600 °C in Comparison to Literature Data for Pure Feedstocks**

| | co-feed (this study) | | | date palm[26] | | | date palm waste[22] | salicornia[41] | |
|---|---|---|---|---|---|---|---|---|---|
| | 400 °C | 500 °C | 600 °C | 400 °C | 500 °C | 600 °C | 550 °C | seed 550 °C | seedless plant 550 °C |
| *Proximate Analysis* | | | | | | | | | |
| moisture (%) | 5.67 | 5.52 | 3.65 | 3.13 | 2.96 | 3.35 | 2.43 | 3.89 | 1.71 |
| volatiles (%) | 24.12 | 14.73 | 10.61 | 20.25 | 9.31 | 6.85 | 22.71 | 40.9 | 16.42 |
| fixed carbon (%) | 30.12 | 34.63 | 38.12 | 63.41 | 71 | 72.44 | 64.77 | 20.54 | 39.96 |
| ash % | 40.09 | 45.12 | 47.62 | 16.34 | 19.68 | 20.71 | 10.09 | 34.67 | 41.91 |
| *Ultimate Analysis* | | | | | | | | | |
| C (%) | 39.77 | 39.88 | 42.08 | 66.87 | 72.3 | 72.89 | | 53.26 | 49.61 |
| H (%) | 1.58 | 1.25 | 0.81 | 3.54 | 2.11 | 1.74 | | 3.94 | 2.89 |
| N (%) | 1.08 | 1.03 | 0.96 | 0.45 | 0.42 | 0.39 | | 2.35 | 0.39 |
| S (%) | 0.15 | 0.18 | 0.21 | 1.36 | 1.02 | 0.98 | | | |
| O (%) | 17.34 | 12.55 | 8.32 | 11.44 | 4.5 | 3.28 | | 5.78 | 5.61 |
| H/C | 0.48 | 0.38 | 0.23 | 0.63 | 0.35 | 0.28 | | 0.89 | 0.71 |

**Table 5. Co-Pyrolized PCM HHV, Surface Area (BET), Acidity, Salinity, and Conductivity at 400, 500, and 600 °C**

| | co-feed (this study) | | | salicornia[41] | | date palm[a52] | | |
|---|---|---|---|---|---|---|---|---|
| | 400 °C | 500 °C | 600 °C | seed 550 °C | seedless 550 °C | 400 °C | 500 °C | 600 °C |
| HHV (MJ/kg) | 16.8 | 17.2 | 16.3 | 22.5 | 16.6 | | 24[b] | |
| BET ($m^2$/kg) | 4.64 | 6.5 | 7.69 | | | | | |
| acidity (pH) | 9.37 | 9.73 | 10.69 | 7.46 | 11.27 | 8.22 | 8.40 | 8.75 |
| salinity (ppt) | 28 | 30.74 | 29.85 | 25.41 | 29.65 | | | |
| conductivity (mS/cm) | 43.16 | 47.20 | 45.85 | 34.52 | 45.67 | 6.67 | 7.53 | 8.07 |

[a]Date palm tree residue, comprising frond midrib and frond base, was subjected to pyrolysis in a stainless-steel container within an electric muffle furnace for 4 h to produce biochar. [b]Auger reactor, Biochar at 525 °C.[17]

H/C ratio, provides insights into the affect of pyrolysis temperature on the biochar characteristics. The observed trend indicates a systematic alteration in the elemental composition of the char with increasing the pyrolysis temperature. Specifically, the H, O, and N contents exhibited a decreasing trend as the pyrolysis temperature increased. This phenomenon is attributed to the removal of oxygen and hydrogen-containing surface functional groups through dehydration.[35] The sulfur content was generally low across all samples, with values ranging from 0.15 to 0.35%. Conversely, the C content in the biochar increased with escalating pyrolysis temperature, rising from 33.67% in the feedstock to 39.77−42.08% in the biochar samples. As shown in Table 4, the C content in the biochar samples is less than 50% for the co-feed; therefore, according to the European Biochar Certificate (EBC) guidelines, this shall be referred to as pyrogenic carbonaceous material (PCM) in the rest of this paper. The observed rise in carbon content after pyrolysis reflects the transformation of feedstock into more carbon-rich structures.[36,47−49] This also increases the PCM stability and benefits carbon sequestration and soil amendment. Similarly, the observed reduction in oxygen and hydrogen contents further enhances the stability, as the removal of these elements implies a drop in labile functional groups and a rise in aromatic carbon structures.[35]

The HHV, pH, and surface area (BET analysis) of the co-feed PCM at three different temperatures are shown in Table 5. The HHV was 16.8, 17.2, and 16.3 MJ/kg at 400, 500, and 600 °C, correspondingly. The HHV of the PCM exceeded that of the feedstock reported in Table 3, which has an HHV of 14.93 MJ/kg. The potential application of PCM for energy generation largely depends on its HHV.[17] The process of pyrolysis enhances the carbon concentration in biochar, thereby increasing its HHV. However, in cases where the feedstock contains excessive ash, the HHV of the resulting PCM decreases, reducing its potential as a solid fuel. However, PCM can offer significant value as a soil modification, particularly in improving the fertility of poor soils. The ash content serves as a source of essential nutritional elements for plant growth and reproduction, such as _P, _K, _Ca, and_Na.

The BET analysis reveals that the surface area of the PCM expands as the temperature rises. These results align with previous studies, where it is reported that higher pyrolysis temperature enhanced the PCM pore size and specific surface area while reducing the PCM yield.[50,51] The PCM acidity, salinity, and electrical conductivity are crucial parameters that prompt potential applications of PCM as a soil amendment and its ability to adjust the pH level in soils. The evaluation of these interrelated properties provides valuable insights into the effectiveness of PCM in agricultural and environmental contexts. The pH levels of PCM are crucial in assessing its appropriateness for various soil compositions. The pH and salinity of the PCM demonstrate an increase in pH after undergoing pyrolysis at various temperatures (Table 5). The pH values measured were 9.37, 9.73, and 10.69 at 400, 500, and 600 °C, respectively. This transformation can be attributed to the breakdown of organic compounds during the pyrolysis process, leading to the release of acidic components and the concentration of ash, which consists of metallic compounds. The increase in alkalinity of PCM after pyrolysis has been well-documented in the literature.[34] This change is noteworthy because alkaline PCM can influence soil quality either positively or negatively depending on the circumstances.

Salinity refers to the concentration of salts present in the PCM. The concentrations of salinity and electrical conductivity increased with increasing temperature of pyrolysis, indicating an increased salt content in the PCM, leading to enhanced ion


https://doi.org/10.1021/acsomega.4c02972
ACS Omega 2024, 9, 24082−24094

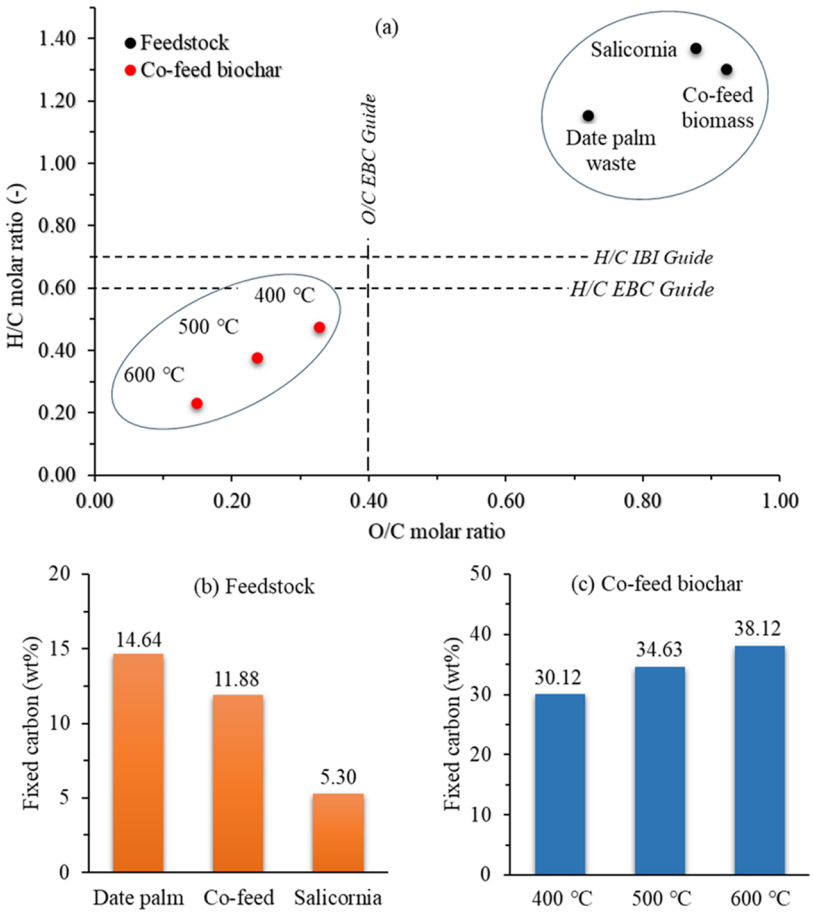


**Figure 7.** Stability in terms of H/C and O/C molar ratios and fixed carbon. The data represent the feedstock and PCM produced from co-feed of date palm waste and Salicornia at 400, 500 and 600 °C.

exchange and greater conductivity. Consequently, the conductivity of the soil can increase when PCM is applied, facilitating the movement of nutrients and ions, which can benefit plant growth. However, it is crucial to exercise caution when using this PCM in soil that is saline by nature. Prolonged application of PCM with elevated salinity can potentially result in soil contamination with heavy metals and extreme salt accumulation. This is particularly relevant in sandy desert areas, where the soil is already naturally high in pH and rich in minerals. In such environments, an excessive rise in salinity over time can hinder plant growth and negatively impact soil health. Furthermore, the arid conditions of deserts pose additional challenges with regard to soil leaching. With limited rainfall and high temperatures, leaching of excess salts from the soil becomes minimal, ans exacerbating the potential risks associated with the PCM-induced salinity increases. Therefore, careful consideration should be given to the specific soil conditions and environmental factors before implementing PCM as a soil amendment, particularly in regions susceptible to salinity and low leaching rates.

*3.4.2. Stability and Carbon Capture Potentials.* The molar ratio of H/C and O/C serves as an indicator of PCM stability, with the European Biochar Certificate (EBC) establishing thresholds of H/C < 0.7[53] and O/C < 0.4[53] for stability. Another metric for assessing stability is the fixed carbon content, which reflects the degree of carbonization and the potential for long-term carbon sequestration.[54] In the data presented in Figure 7, PCM produced from co-feed processes at 400, 500, and 600 °C consistently falls within the stability thresholds set by IBI and EBC. Increasing pyrolysis temperature correlates with increased PCM stability, as evidenced by lower H/C and O/C ratios (e.g., co-feed biochar at 600 °C (H/C = 0.23, O/C = 0.15)) and higher fixed carbon percentages (38.12%). Comparatively, the feedstocks exhibit instability, characterized by O/C ratios exceeding 0.4 and H/C ratios surpassing 0.6, along with limited fixed carbon; however, the co-feed PCM demonstrates stability suitable for long-term carbon sequestration, indicating its potential superiority over individual biomass usage. The stability of PCM is positively associated with its fixed carbon content, as demonstrated by comparison with pure biomass samples. Overall, pyrolysis shifts original biomass toward the lower left corner of the stability plot, aligning with IBI and EBC guidelines.

**3.5. Bio-Oil (Organic Phase) Properties.** *3.5.1. Bio-Oil Chemical Composition.* The organic composition of the resulting heavy-phase bio-oil was determined by utilizing a GC/MS system. The findings are presented as a percentage of the total area for the detected compounds as shown in Table 6 for the main ten compounds (the full list of compounds is shown in Tables S1−S3). At 400 °C, notable compounds include (1,4,4-trimethyl-cyclohex-2-enyl)-acetic acid, phenol, and 4-tetradecene, constituting 5.44, 4.92, and 4.22% of the bio-oil, respectively. As the temperature rises to 500 °C, a shift in the composition is observed, with 1-tetradecene, cetene, and 3-cyclopropenoic acid,1-butyl, methyl ester emerging as predominant components, accounting for 12.09, 7.07, and


https://doi.org/10.1021/acsomega.4c02972
ACS Omega 2024, 9, 24082−24094

**Table 6. GCMS Compounds Name List of Bio-Oil Produced at 400, 500, and 600 °C**

| compound name | area (%) |
|---|---|
| 400 °C Bio-Oil | |
| (1,4,4-trimethyl-cyclohex-2-enyl)-acetic acid | 5.44 |
| phenol, 2,6-dimethoxy- | 4.92 |
| 4-tetradecene, (*Z*)- | 4.22 |
| carbamic acid, (3-methylphenyl)-, 3-[(methoxycarbonyl)amino]phenyl ester | 3.51 |
| 1-tetradecene | 3.31 |
| 2-propenal, 3-(2-nitrophenyl)- | 3.01 |
| phenol | 2.86 |
| mandelic acid | 2.67 |
| 1-heptacosanol | 2.6 |
| hexatriacontane | 2.53 |
| 500 °C Bio-Oil | |
| 1-tetradecene | 12.09 |
| cetene | 7.07 |
| 3-cyclopropenoic acid,1-butyl, methyl ester | 6.16 |
| *n*-tetracosanol-1 | 5.66 |
| carbamic acid, phenyl ester | 5.42 |
| 1-tridecene | 5.36 |
| dodecane, 1-chloro- | 4.56 |
| 4H-1,2,4-triazole-4-amine, *N*-[(2-nitrophenyl)methylene]- | 3.62 |
| 4-methyl-2-propyl-1-pentanol | 3.61 |
| phenol, 2,2′-methylenebis[6-(1,1-dimethylethyl)-4-methyl]- | 2.73 |
| 600 °C Bio-Oil | |
| 1-pentadecene | 4.95 |
| 3-tetradecene, (*E*)- | 4.44 |
| methanesulfinylbenzene | 4.22 |
| 10-heneicosene (c,t) | 3.36 |
| 1-tridecene | 3.19 |
| 1-hexadecanol | 3.04 |
| octadecane, 1-(ethenyloxy)- | 3 |
| benzene, 4-methyl-1,2-dinitro- | 2.47 |
| phenol, 2,2′-methylenebis[6-(1,1-dimethylethyl)-4-methyl]- | 2.28 |
| heneicosanoic acid, methyl ester | 2.13 |

6.16% of the bio-oil, respectively. Additionally, compounds like *n*-tetracosanol-1 and 1-tridecene show significant presence at this temperature. At the highest temperature of 600 °C, the composition further evolves, with 1-pentadecene, 3-tetradecene, and methanesulfinylbenzene being prominent, making up 4.95, 4.44, and 4.22% of the bio-oil, respectively. Notably, certain compounds, such as phenol, 2,2′-methylenebis[6-(1,1-dimethylethyl)-4-methyl-], appear consistently across different temperature regimes, albeit at varying proportions. These findings underscore the temperature-dependent nature of bio-oil composition during pyrolysis and highlight the potential for tailored production of bio-oil with desired chemical profiles.

The results depict a composition rich in both saturated and unsaturated hydrocarbons. Saturated hydrocarbons consist of carbon atoms bonded by single bonds such as alkanes. Unsaturated hydrocarbons, on the other hand, contain at least one double or triple carbon−carbon bond, such as in alkenes and alkynes.[55,56] Based on the detected compounds, the composition of the bio-oil is grouped as shown in Figure 8. The saturated and unsaturated hydrocarbons varying in concentration between 25 and 36% in terms of area percentage. The selectivity toward these hydrocarbons exhibited a pattern of 35.3% at 500 °C > 33.03% at 600 °C > 25.5% at 400 °C. During the process, the decarboxylation of carboxylic acids occurred, resulting in the generation of $CO_2$, alongside a significant presence of ester hydrocarbons. The selectivity toward ester hydrocarbons decreased from 24.2% at 400 °C to 15.07% at 600 °C, possibly attributed to cracking at higher temperatures, causing volatiles to convert into NCG gases such as $CO_2$ and lighter hydrocarbons. The presence of proteins in the material influenced the generation of diverse nitrogen-containing compounds. Amino acids, constituting proteins, contributed to the creation of nitrogen-containing heterocyclic chemicals such as cyano/nitriles and amines/amides. The selectivity toward N-aromatic compounds peaked at 600 °C (7.1%), followed by 6.54% at 500 °C and 3.62% at 400 °C, attributed to increased cyclization and aromatization reactions at higher pyrolysis temperatures. A comparable pattern was previously noted and documented by Kuttiyathil et

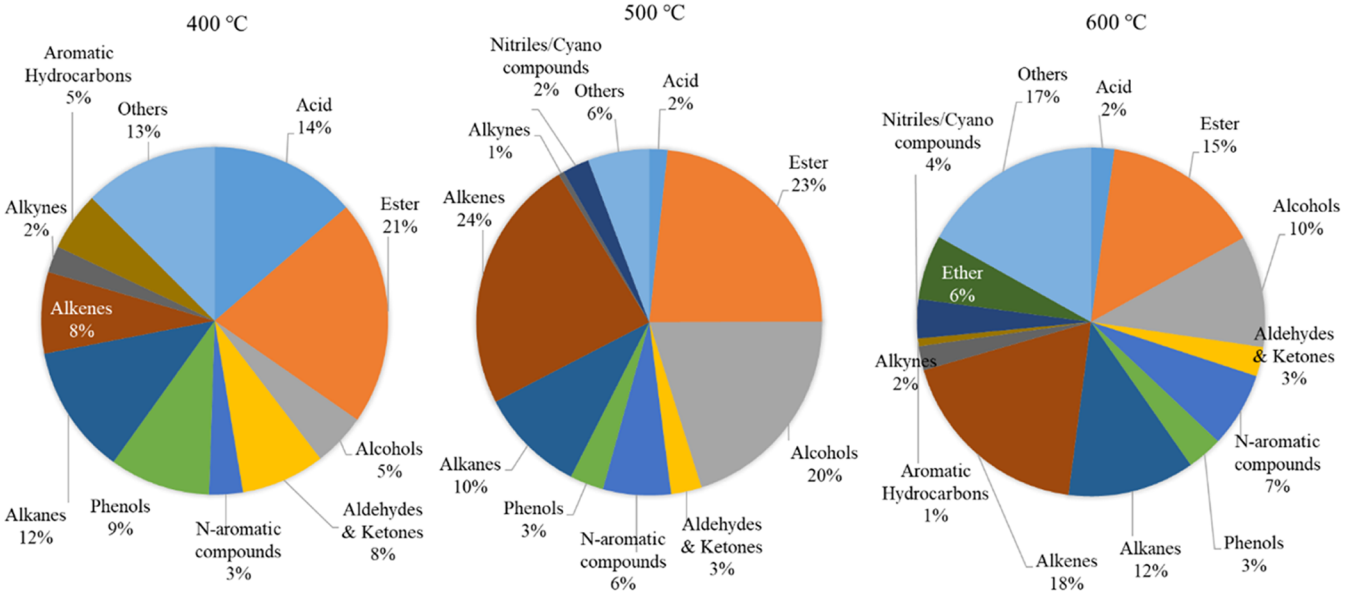


**Figure 8.** Chemical composition of co-feed heavy-phase bio-oil produced at 400, 500 and 600 °C.



https://doi.org/10.1021/acsomega.4c02972
*ACS Omega* 2024, 9, 24082−24094

al.[57] The existence of cellulose fiber and hemicellulose in the biomass led to the production of low-molecular-weight carbonyl compounds, such as aldehydes and ketones. Secondary reactions and the transformation of levoglucosan resulted in additional low-molecular-weight oxygenates and noncondensable gases, favored by the pyrolysis temperatures and vapor residence times. The bio-oil demonstrated selectivity of 9.01, 2.95, and 2.76% toward furan derivatives at 400, 500, and 600 °C, correspondingly. Ketone molecules identified in the bio-oil were mainly 2-cyclopenten-1-one structures, which are common byproducts of cellulose and hemicellulose pyrolysis. The concentration of ketones decreased with increasing temperatures, aligning with prior findings from the literature.[58]

Phenolic chemicals detected in the bio-oil are primarily sourced from lignin, a biopolymer composed of phenylpropanoid monomers linked via C−O and C−C linkages. The selectivity toward phenolics decreased with increasing temperature: 10.84% at 400 °C > 3.25% at 500 °C < 3.36% at 600 °C. The phenols produced from the pyrolysis of phenylalanine and other amino acids included phenol and 2,6-dimethoxy-phenol. Phenolics are also responsible for synthesizing aromatic hydrocarbons through deoxygenation. Pyrolysis typically results in bio-oil with high oxygen content due to various oxygenated compounds like aldehydes, ketones, acids, and phenolics present during the process. However, the existence of these oxygenated compounds can lead to bio-oil instability and engine corrosion, reducing the attractiveness of bio-oil as a fuel. The bio-oil also had high-water content and extreme acidity, which could cause corrosion and instability during storage and emissions of nitrogen oxides ($NO_x$) after burning. To utilize crude bio-oil as a feedstock for transportation fuel, it would be necessary to remove these oxygenated and nitrogenated species. Conversely, the compounds identified as most abundant in the bio-oil has the potential to act as antioxidants, potentially minimizing reactive oxygen. These compounds might serve as antioxidants in the bio-oil itself or when blended with biodiesel to enhance stability. Moreover, these chemicals could be isolated and utilized commercially as antioxidants in various biolubricants.

*3.5.2. Pyrolysis Liquid HHV and Acidity.* The HHV of the co-feed pyrolysis liquid (organic phase bio-oil and aqueous phases) is presented in Table 7. The results were 32.29 36.29, and 33.73 MJ/kg at 400, 500, and 600 °C, correspondingly. These values are within the high range compared with bio-oil produced from woody feedstocks. Moreover, the obtained results were higher than the reported HHV for bio-oil for pure date palm waste bio-oil (20.88 MJ/kg at 550 °C) and from Salicornia seed and seedless plant bio-oil samples produced at 550 °C (24.9 and 29.3 MJ/kg, correspondingly). These findings indicate that the co-feed mixture yields bio-oil with higher HHV content than pure feedstock. This highlights the advantage of combining different biomass sources to optimize the HHV of the final bio-oil. The acidity of the bio-oils generated through pyrolysis is observed to vary with the temperature changes. Bio-oils from date palm and seedless Salicornia exhibit acidity, typical of acidic substances.[17] However, the presence of seeds contributes to increased alkalinity compared with pure date palm. The acidity levels are notably low for heavy and aqueous phases in the co-feed bio-oil. In contrast, bio-oils from *S. bigelovii* seedless, date palm waste, and other lignocellulosic biomass are acidic with a pH below 6, similar to values reported in the literature for bio-oils from woody biomass or general agricultural waste.[17,28,41] Due to their lipid-rich nature, Salicornia seeds produce bio-oils with a pH equal to or greater than 6.[17] The aqueous phases of the co-feed bio-oils have a high-water content of approximately 71−72%. At the highest temperature 600 °C, the pH of the heavy and light phases bio-oil recorded the highest values of 4.39 and 4.18, respectively. However, bio-oils directly obtained from pyrolysis may be difficult to use as fuels and therefore lack significant commercial value without additional improvement. This is attributed to their high oxygen content, poor stability, and corrosivity. The challenge with bio-oils from lignocellulosic biomass lies in their complex composition, comprising aldehydes, aliphatic, ketones, aromatic alcohols, carboxylic acids, ethers, and phenolic derivatives. Addressing these challenges necessitates the ex situ removal of oxygen through processes such as hydro-deoxygenation, alongside mechanistic pathways involving hydrocracking and hydro-isomerization reactions.[57]

**Table 7. Co-Feed Pyrolysis Liquid (Organic and Aqueous Phases) HHV and Acidity Produced at 400, 500, and 600 °C**

| | this study | | | salicornia[41a] | |
|---|---|---|---|---|---|
| | 400 °C | 500 °C | 600 °C | seed 550 °C | seedless 550 °C |
| HHV (organic phase) (MJ/kg) | 32.29 | 36.29 | 33.73 | 24.89 | 29.28 |
| pH (organic Phase) | 4.17 | 3.76 | 4.39 | 8.5 | 5.2 |
| pH (aqueous Phase) | 3.44 | 3.73 | 4.18 | 9.6 | 4.9 |

[a]Auger reactor.

## 4. CONCLUSIONS

This research introduces the first experimental analysis of the co-feed pyrolysis of date palm waste and *S. Bigelovii* within the temperature range of 400−600 °C. Both types of feedstocks are classified under halophyte plants and are expected to significantly contribute to advancing bioenergy development in xeric regions. The quality of the feedstocks and pyrolysis product distribution were compared to the pure feedstock cases. The impact of the pyrolysis temperature was found to follow the classic trend reported in the pyrolysis literature, where the PCM decreases, while the gas increases with increasing pyrolysis temperatures. The co-feed produced moderate bio-oil yield (∼19.9 mass%) with high calorific value (average HHV = 34.1 MJ/kg). The hydrogen in the NCG increased significantly with temperature, leading to a substantial increase in the NCG HHV (24.12 MJ/kg at 600 °C), influenced by the increased ash catalytic effect at high temperature. The PCM produced from within the temperature range of 400−600 °C has an average HHV of 16.7 MJ/kg and an average acidity of pH = 9.93. The PCM has also been found to be high in ash due to the nature of the feedstock. This PCM may find better application as a soil amendment; however, the long-term impact of such an alkaline and high ash PCM in naturally alkaline soil, such as in xeric soil, should be treated with caution. Moreover, increased pyrolysis temperature is confirmed to enhance the PCM stability, as evidenced by low H/C and O/C molar ratios and increased fixed carbon percentages, aligning with EBC and IBI guidelines and suggesting the superiority of co-feed PCM over individual biomass usage. Finally, these findings demonstrate the potential of co-feeding date palm waste with *S. biggilovii* as a


https://doi.org/10.1021/acsomega.4c02972
ACS Omega 2024, 9, 24082−24094

sustainable method for waste management while producing renewable energy and PCM. Moreover, while the potential of co-pyrolysis for sustainable energy and soil enhancement is promising, further research into the potential toxicological impacts of PCM as a soil amendment is essential to ensure its safe and effective utilization.

## ■ ASSOCIATED CONTENT

### Supporting Information

The Supporting Information is available free of charge at https://pubs.acs.org/doi/10.1021/acsomega.4c02972.

GCMS chemical composition of bio-oil at 400 °C (Table S1); GCMS chemical composition of bio-oil at 500 °C (Table S2); GCMS chemical composition of bio-oil at 600 °C (Table S3) (PDF)

## ■ AUTHOR INFORMATION


### Corresponding Authors

**Yassir Makkawi** − *Bioenergy and Solar Conversion Research Group (BSCRG), College of Engineering, American University of Sharjah, 26666 Sharjah, UAE;* orcid.org/0000-0003-0260-0192; Phone: +97165152167; Email: ymakkawi@aus.edu; Fax: +97165152979

**Fatin Samara** − *Department of Biology, Chemistry and Environmental Science, American University of Sharjah, 26666 Sharjah, UAE*; Phone: +97165152440; Email: fsamara@aus.edu

### Author

**Waqas Ahmad** − *Materials Science and Engineering Program, College of Arts and Sciences, American University of Sharjah, 26666 Sharjah, UAE; Bioenergy and Solar Conversion Research Group (BSCRG), College of Engineering, American University of Sharjah, 26666 Sharjah, UAE*

Complete contact information is available at: https://pubs.acs.org/10.1021/acsomega.4c02972


### Notes

The authors declare no competing financial interest.

## ■ ACKNOWLEDGMENTS

The authors would like to acknowledge the American University of Sharjah (AUS) for providing financial support (ref: FRG23-C-E33). Mr. Waqas Ahmad acknowledges the AUS admission to the Materials Science and Engineering PhD Program at AUS.

## ■ REFERENCES


(1) Ussiri, D. A. N.; Lal, R. Carbon Sequestration for Climate Change Mitigation and Adaptation. In *Carbon Sequestration for Climate Change Mitigation and Adaptation*; Springer, 2017.

(2) Antar, M.; Lyu, D.; Nazari, M.; Shah, A.; Zhou, X.; Smith, D. L. Biomass for a Sustainable Bioeconomy: An Overview of World Biomass Production and Utilization. *Renewable Sustainable Energy Rev.* **2021**, *139*, No. 110691.

(3) Gielen, D.; Boshell, F.; Saygin, D.; Bazilian, M. D.; Wagner, N.; Gorini, R. The Role of Renewable Energy in the Global Energy Transformation. *Energy Strategy Rev.* **2019**, *24*, 38−50.

(4) European Commission. Energy for The Future: Renewable Sources Of Energy. 1997.

(5) Sun, Y.; Gao, B.; Yao, Y.; Fang, J.; Zhang, M.; Zhou, Y.; Chen, H.; Yang, L. Effects of Feedstock Type, Production Method, and Pyrolysis Temperature on Biochar and Hydrochar Properties. *Chem. Eng. J.* **2014**, *240*, 574−578.

(6) Song, W.; Guo, M. Quality Variations of Poultry Litter Biochar Generated at Different Pyrolysis Temperatures. *J. Anal. Appl. Pyrolysis* **2012**, *94*, 138−145.

(7) Shanmugam, V.; Sreenivasan, S. N.; Mensah, R. A.; Försth, M.; Sas, G.; Hedenqvist, M. S.; Neisiany, R. E.; Tu, Y.; Das, O. A Review on Combustion and Mechanical Behaviour of Pyrolysis Biochar. *Mater. Today Commun.* **2022**, *31*, No. 103629.

(8) Gai, X.; Wang, H.; Liu, J.; Zhai, L.; Liu, S.; Ren, T.; Liu, H. Effects of Feedstock and Pyrolysis Temperature on Biochar Adsorption of Ammonium and Nitrate. *PLoS One* **2014**, *9* (12), No. 0113888.

(9) Liu, Z.; Jia, M.; Li, Q.; Lu, S.; Zhou, D.; Feng, L.; Hou, Z.; Yu, J. Comparative Analysis of the Properties of Biochars Produced from Different Pecan Feedstocks and Pyrolysis Temperatures. *Ind. Crops Prod.* **2023**, *197*, No. 116638.

(10) Lee, X. J.; Ong, H. C.; Gan, Y. Y.; Chen, W. H.; Mahlia, T. M. I. State of Art Review on Conventional and Advanced Pyrolysis of Macroalgae and Microalgae for Biochar, Bio-Oil and Bio-Syngas Production. *Energy Convers. Manage.* **2020**, *210*, No. 112707.

(11) Peng, C.; Feng, W.; Zhang, Y.; Guo, S.; Yang, Z.; Liu, X.; Wang, T.; Zhai, Y. Low Temperature Co-Pyrolysis of Food Waste with PVC-Derived Char: Products Distributions, Char Properties and Mechanism of Bio-Oil Upgrading. *Energy* **2021**, *219*, No. 119670.

(12) Ly, H. V.; Lee, B.; Sim, J. W.; Tran, Q. K.; Kim, S. S.; Kim, J.; Brigljević, B.; Hwang, H. T.; Lim, H. Catalytic Pyrolysis of Spent Coffee Waste for Upgrading Sustainable Bio-Oil in a Bubbling Fluidized-Bed Reactor: Experimental and Techno-Economic Analysis. *Chem. Eng. J.* **2022**, *427*, No. 130956.

(13) Awad, S.; Zhou, Y.; Katsou, E.; Li, Y.; Fan, M. A Critical Review on Date Palm Tree (Phoenix Dactylifera L.) Fibres and Their Uses in Bio-Composites. *Waste Biomass Valorization* **2021**, *12*, 2853−2887.

(14) Chao, C. C. T.; Krueger, R. R. The Date Palm (Phoenix Dactylifera L.): Overview of Biology, Uses, and Cultivation. *HortScience* **2007**, *42* (5), 1077−1082.

(15) Bastidas-Oyanedel, J. R.; Fang, C.; Almardeai, S.; Javid, U.; Yousuf, A.; Schmidt, J. E. Waste Biorefinery in Arid/Semi-Arid Regions. *Bioresour. Technol.* **2016**, *215*, 21−28.

(16) Makkawi, Y.; Pour, F. H.; Moussa, O.Case Study in Arid and Semi-Arid Regions. In *Waste-to-Energy*; Springer, 2022; pp 577−612.

(17) Makkawi, Y.; Khan, M.; Pour, F. H.; Moussa, O.; Mohamed, B.; Alnoman, H.; Elsayed, Y. A Comparative Analysis of Second-Generation Biofuels and Its Potentials for Large-Scale Production in Arid and Semi-Arid Regions. *Fuel* **2023**, *343*, No. 127893.

(18) Al-Wabel, M. I.; Usman, A. R. A.; Al-Farraj, A. S.; Ok, Y. S.; Abduljabbar, A.; Al-Faraj, A. I.; Sallam, A. S. Date Palm Waste Biochars Alter a Soil Respiration, Microbial Biomass Carbon, and Heavy Metal Mobility in Contaminated Mined Soil. *Environ. Geochem. Health* **2019**, *41* (4), 1705−1722.

(19) Ramadan, M. F.; Farag, M. A.*Mediterranean Fruits Bio-wastes: Chemistry, Functionality and Technological Applications*; Springer, 2022.

(20) Ben Salem, I.; El Gamal, M.; Sharma, M.; Hameedi, S.; Howari, F. M. Utilization of the UAE Date Palm Leaf Biochar in Carbon Dioxide Capture and Sequestration Processes. *J. Environ. Manage.* **2021**, *299*, No. 113644.

(21) El-Mously, H.; Midani, M.; Darwish, E. A. *Date Palm Byproducts: A Springboard for Circular Bio Economy.*; Springer, 2023.

(22) Makkawi, Y.; El Sayed, Y.; Salih, M.; Nancarrow, P.; Banks, S.; Bridgwater, T. Fast Pyrolysis of Date Palm (Phoenix Dactylifera) Waste in a Bubbling Fluidized Bed Reactor. *Renewable Energy* **2019**, *143*, 719−730.

(23) Bastidas-Oyanedel, J. R.; Schmidt, J. E.*Biorefinery: Integrated Sustainable Processes for Biomass Conversion to Biomaterials, Biofuels, and Fertilizers*; Springer, 2019.

(24) Nasser, R. A. Date Palm for Energy Production. *BioResources* **2014**, *9* (3), 4343−4357.

(25) Bañuelos, J. A.; Velázquez-Hernández, I.; Guerra-Balcázar, M.; Arjona, N. Production, Characterization and Evaluation of the




https://doi.org/10.1021/acsomega.4c02972
*ACS Omega* 2024, 9, 24082−24094

Energetic Capability of Bioethanol from *Salicornia Bigelovii* as a Renewable Energy Source. *Renewable Energy* **2018**, *123*, 125−134.
(26) Usman, A. R. A.; Abduljabbar, A.; Vithanage, M.; Ok, Y. S.; Ahmad, M.; Ahmad, M.; Elfaki, J.; Abdulazeem, S. S.; Al-Wabel, M. I. Biochar Production from Date Palm Waste: Charring Temperature Induced Changes in Composition and Surface Chemistry. *J. Anal. Appl. Pyrolysis* **2015**, *115*, 392−400.
(27) Ahmad, M.; Ahmad, M.; Usman, A. R. A.; Al-Faraj, A. S.; Abduljabbar, A.; Ok, Y. S.; Al-Wabel, M. I. Date Palm Waste-Derived Biochar Composites with Silica and Zeolite: Synthesis, Characterization and Implication for Carbon Stability and Recalcitrant Potential. *Environ. Geochem. Health* **2019**, *41* (4), 1687−1704.
(28) Burezq, H.; Davidson, M. K. Biochar from Date Palm (Phoenix Dactylifera L.) Residues—a Critical Review. *Arabian J. Geosci.* **2023**, *16* (2), No. 101.
(29) Falasca, S. L.; Ulberich, A.; Acevedo, A. Identification of Argentinian Saline Drylands Suitable for Growing *Salicornia Bigelovii* for Bioenergy. *Int. J. Hydrogen Energy* **2014**, *39*, 8682−8689.
(30) Alsulami, R. A.; El-Sayed, S. A.; Eltaher, M. A.; Mohammad, A.; Almitani, K. H.; Mostafa, M. E. Thermal Decomposition Characterization and Kinetic Parameters Estimation for Date Palm Wastes and Their Blends Using TGA. *Fuel* **2023**, *334*, No. 126600.
(31) Dzidzienyo, P.; Bastidas-Oyanedel, J. R.; Schmidt, J. E. Pyrolysis Kinetics of the Arid Land Biomass Halophyte *Salicornia Bigelovii* and Phoenix Dactylifera Using Thermogravimetric Analysis. *Energies* **2018**, *11* (9), No. 2283.
(32) Sait, H. H.; Hussain, A.; Bassyouni, M.; Ali, I.; Kanthasamy, R.; Ayodele, B. V.; Elhenawy, Y. Hydrogen-Rich Syngas and Biochar Production by Non-Catalytic Valorization of Date Palm Seeds. *Energies* **2022**, *15* (8), No. 2727.
(33) Shahmirzadi, A. N.; Najafi, S. K.; Younesi, H. Potential Assessment of Hybrid Biochar from the Date Palm and Pistachio Residues. *J. Wood Chem. Technol.* **2022**, *42* (6), 435−444.
(34) Sizirici, B.; Fseha, Y. H.; Yildiz, I.; Delclos, T.; Khaleel, A. The Effect of Pyrolysis Temperature and Feedstock on Date Palm Waste Derived Biochar to Remove Single and Multi-Metals in Aqueous Solutions. *Sustainable Environ. Res.* **2021**, *31* (1), No. 9.
(35) Iaccarino, A.; Gautam, R.; Sarathy, S. M. Bio-Oil and Biochar Production from Halophyte Biomass: Effects of Pre-Treatment and Temperature on *Salicornia Bigelovii* Pyrolysis. *Sustainable Energy Fuels* **2021**, *5* (8), 2234−2248.
(36) Aljaziri, J.; Gautam, R.; Sarathy, S. M. Interactions in Co-Pyrolysis of *Salicornia Bigelovii* and Heavy Fuel Oil †. *Sustainable Energy Fuels* **2023**, *7*, 4213−4228.
(37) Al Marzooqi, F.; Yousef, L. F. Biological Response of a Sandy Soil Treated with Biochar Derived from a Halophyte (*Salicornia Bigelovii*). *Appl. Soil Ecol.* **2017**, *114*, 9−15.
(38) Shahid, M.; Jaradat, A. A.; Rao, N. K. Use of Marginal Water for *Salicornia Bigelovii* Torr. Planting in the United Arab Emirates. In *Developments in Soil Salinity Assessment and Reclamation*; Springer: Netherlands, 2013; pp 451−462.
(39) Soltani, I.; Berrich, E.; Romdhane, M.; Fethi, A. Heating Rate and ZSM-5 Catalyst Effects on Date Palm (Phoenix Dactylifera L.) Stones Pyrolysis: Thermogravimetric Analysis, Production and Characterization of Syngases and Bio-Oils. *J. Energy Inst.* **2023**, *110*, No. 101295.
(40) Makkawi, Y.; Hassan Pour, F.; Elsayed, Y.; Khan, M.; Moussa, O.; Masek, O.; Badrelzaman, M.; El Tahir, W. Recycling of Post-Consumption Food Waste through Pyrolysis: Feedstock Characteristics, Products Analysis, Reactor Performance, and Assessment of Worldwide Implementation Potentials. *Energy Convers. Manage.* **2022**, *272*, No. 116348.
(41) Makkawi, Y.; El Sayed, Y.; Lyra, D. A.; Pour, F. H.; Khan, M.; Badrelzaman, M. Assessment of the Pyrolysis Products from Halophyte *Salicornia Bigelovii* Cultivated in a Desert Environment. *Fuel* **2021**, *290*, No. 119518.
(42) Bensidhom, G.; Ben Hassen-Trabelsi, A.; Alper, K.; Sghairoun, M.; Zaafouri, K.; Trabelsi, I. Pyrolysis of Date Palm Waste in a Fixed-Bed Reactor: Characterization of Pyrolytic Products. *Bioresour. Technol.* **2017**, *247*, 363−369.
(43) Lukáš Gašparovič, Z. K. L'. J. In *Kinetic Study of Wood Chips Decomposition by TGA*, 36th International Conference of Slovak Society of Chemical EngineeringMarkoš, J.Slovak Society of Chemical Engineering: Tatransk'e Matliare: Slovakia, 2009.
(44) Nasser, R. A.; Salem, M. Z. M.; Hiziroglu, S.; Al-Mefarrej, H. A.; Mohareb, A. S.; Alam, M.; Aref, I. M. Chemical Analysis of Different Parts of Date Palm (Phoenix Dactylifera L.) Using Ultimate, Proximate and Thermo-Gravimetric Techniques for Energy Production. *Energies* **2016**, *9* (5), No. 374.
(45) Sait, H. H.; Hussain, A.; Salema, A. A.; Ani, F. N. Pyrolysis and Combustion Kinetics of Date Palm Biomass Using Thermogravimetric Analysis. *Bioresour. Technol.* **2012**, *118*, 382−389.
(46) Acharya, S.; Wang, T. Exploration of Recovering Waste Heat in a Cascade Liquefied Natural Gas (LNG) Plant, ASME International Mechanical Engineering Congress and Exposition; ASME, 2024.
(47) Rutherford, D. W.; Wershaw, R. L.; Rostad, C. E.; Kelly, C. N. Effect of Formation Conditions on Biochars: Compositional and Structural Properties of Cellulose, Lignin, and Pine Biochars. *Biomass Bioenergy* **2012**, 693−701.
(48) Irfan, M.; Chen, Q.; Yue, Y.; Pang, R.; Lin, Q.; Zhao, X.; Chen, H. Co-Production of Biochar, Bio-Oil and Syngas from Halophyte Grass (Achnatherum Splendens L.) under Three Different Pyrolysis Temperatures. *Bioresour. Technol.* **2016**, *211*, 457−463.
(49) Iaccarino, A.; Gautam, R.; Sarathy, S. M. Bio-Oil and Biochar Production from Halophyte Biomass: Effects of Pre-Treatment and Temperature On *Salicornia Bigelovii* pyrolysis. *Sustainable Energy Fuels* **2021**, *5* (8), 2234−2248.
(50) Huang, H.; Reddy, N. G.; Huang, X.; Chen, P.; Wang, P.; Zhang, Y.; Huang, Y.; Lin, P.; Garg, A. Effects of Pyrolysis Temperature, Feedstock Type and Compaction on Water Retention of Biochar Amended Soil. *Sci. Rep.* **2021**, *11* (1), No. 7419.
(51) Wang, H.; Garg, A.; Huang, S.; Mei, G. Mechanism of Compacted Biochar-Amended Expansive Clay Subjected to Drying−Wetting Cycles: Simultaneous Investigation of Hydraulic and Mechanical Properties. *Acta Geophys.* **2020**, *68* (3), 737−749.
(52) Alotaibi, K. D.; Schoenau, J. J. Addition of Biochar to a Sandy Desert Soil: Effect on Crop Growth,Water Retention and Selected Properties. *Agronomy* **2019**, *9* (6), No. 327.
(53) Peter, H. European Biochar Certificate-Guidelines for a Sustainable Production of Biochar. 2012. DOI: 10.13140/RG.2.1.4658.7043.
(54) Leng, L.; Huang, H.; Li, H.; Li, J.; Zhou, W. Biochar Stability Assessment Methods: A Review. *Sci. Total Environ.* **2019**, *647*, 210−222.
(55) Kobayashi, H.; Bell, A. T.; Shen, M. Plasma Polymerization of Saturated and Unsaturated Hydrocarbons. *Macromolecules* **1974**, *7* (3), 277−283.
(56) Bond, G. C.; Wells, P. B. *The Mechanism of the Hydrogenation Hydrocarbons of Unsaturated on Transition Metal Catalysts.*; Elsevier, 1965.
(57) Kuttiyathil, M. S.; Sivaramakrishnan, K.; Ali, L.; Shittu, T.; Z Iqbal, M.; Khaleel, A.; Altarawneh, M. Catalytic Upgrading of Pyrolytic Bio-Oil from *Salicornia Bigelovii* Seeds for Use as Jet Fuels: Exploring the Ex-Situ Deoxygenation Capabilities of Ni/Ze Catalyst. *Bioresour. Technol. Rep.* **2023**, *22*, No. 101437.
(58) Zhao, C.; Jiang, E.; Chen, A. Volatile Production from Pyrolysis of Cellulose, Hemicellulose and Lignin. *J. Energy Inst.* **2017**, *90* (6), 902−913.


https://doi.org/10.1021/acsomega.4c02972
*ACS Omega* 2024, 9, 24082−24094